Evolution of Structures and Stabilities of Zinc-Doped Tin Clusters SnnZn, n = 1–12. Three-dimensional Aromaticity of the Magic Clusters Sn10Zn and Sn12Zn

ARTICLE *in* CHEMICAL PHYSICS · SEPTEMBER 2011

Impact Factor: 1.65 · DOI: 10.1016/j.chemphys.2011.06.041

3 AUTHORS:

Truong Tai
University of Leuven
65 PUBLICATIONS **506** CITATIONS
SEE PROFILE

Tam Minh Nguyen
University of Leuven
20 PUBLICATIONS **136** CITATIONS
SEE PROFILE

Minh Tho Nguyen
University of Leuven
748 PUBLICATIONS **10,846** CITATIONS
SEE PROFILE

Chemical Physics 388 (2011) 1–8

Contents lists available at ScienceDirect

Chemical Physics

journal homepage: www.elsevier.com/locate/chemphys

Evolution of structures and stabilities of zinc-doped tin clusters Sn_nZn, $n = 1–12$. Three-dimensional aromaticity of the magic clusters $Sn_{10}Zn$ and $Sn_{12}Zn$

Truong Ba Tai [a], Nguyen Minh Tam [a,b], Minh Tho Nguyen [a,b,*]

[a] Department of Chemistry, Katholieke Universiteit Leuven, B-3001 Leuven, Belgium
[b] Institute for Computational Science and Technology of HoChiMinh City, Thu Duc, HoChiMinh City, Viet Nam

ARTICLE INFO

Article history:
Received 5 May 2011
In final form 29 June 2011
Available online 22 July 2011

Keywords:
Tin clusters
Zinc-doped tin clusters
Stochastic search
Cluster growth mechanism
Spherical aromaticity

ABSTRACT

Small zinc-doped tin clusters Sn_nZn, $n = 1–12$, are studied using DFT and CCSD(T) methods. The isomers are located using a stochastic search algorithm. The growth mechanism can be formulated as follows: (i) small clusters Sn_nZn with $n \leqslant 8$ are formed by capping Zn on a surface of Sn_n, (ii) a competition between exohedral and endohedral structures appears at $n = 9$ and 10, from which the endohedral structures become predominant, (iii) for $n = 11$ and 12, the clusters are formed by encapsulating Zn into the empty cages Sn_n. Icosahedral $Sn_{12}Zn$ (I_h) and $Sn_{10}Zn$ (D_{4d}) are magic clusters with large HOMO–LUMO gaps, high binding energies and embedding energies. While both $Sn_{12}Zn$ and $Sn_{10}Zn$ clusters can be considered to be spherically aromatic with 8 valence π-electrons that satisfy the electron count rule of $2(N + 1)^2$, the enhanced stability of $Sn_{12}Zn$ (I_h) can further be rationalized in terms of its closed crystal field splitting shell.

1. Introduction

Binary clusters of the elements continue to attract much attention, in part due to their interesting chemical and physical properties. It is known that addition of one impurity into a host results in a new type of clusters whose properties differ basically from those of their parent. This leads to a huge range of impure clusters that constitutes the intriguing subjects for many experimental and theoretical studies.

The clusters based on the group IVA elements have in particular been attractive because of their numerous applications in electronic industries and nanotechnology [1]. During the past decades, a large number of investigations on the geometric structures, thermodynamic stabilities and spectroscopic properties of the pure group IVA clusters [2–15] and impure clusters [16–26] have been performed using various experimental and theoretical methods. It is interesting to note that while the structures of the small pure clusters X_n with X = Si, Ge, Sn and Pb are found to be similar to each other, and can be compared to those of the corresponding boron hydrides B_nH_n, the structures and growth mechanism of the doped clusters turn out to be quite different and depend not only on the nature of the dopants and also on that of the hosts. For instance, Gopakumar et al. [16] showed from calculations that the Li impurity tends to be doped on the surfaces of Ge-hosts and slightly distorts the structures Ge_nLi_m ($n = 1–9$ and $m = 1–2$) as compared to the Ge_n-hosts. Wang and coworkers [22] found that the small transition metal doped germanium clusters Ge_nM (M = Cu, Zn) are formed by substituting one Ge-atom of the Ge_{n+1} core with metal impurities. This growth motif was also observed for the Au-doped germanium clusters [19]. Recently, based on DFT calculations and experimental photoelectron spectrometric results, Clayborne et al. [27] reported that the doped anionic clusters Sn_nBi^- have structures similar to their parent clusters Sn_{n+1}, but in addition exhibit an aromatic character. Additionally, many experimental and theoretical studies on a few special sizes of doped group IVA clusters X_nM, with M = transition metal, and $n = 10$ and 12, pointed out that while metal dopants tend to be located outside of the silicon clusters, they are endohedrally doped into the empty cages of the heavier element clusters X_n, with X = Ge, Sn and Pb [23,24,26,28]. This can be understood in terms of the nature of dopants M and also the size of the empty cages X_n. Moreover, addition of a transition metal atom into group IVA clusters not only improves their stabilities as compared to the host clusters, but also form high symmetry structures that can be used as building blocks for assembling novel nano-materials.

Compared to the silicon- and germanium-based impure clusters, reports on the doped tin clusters are quite limited. According to our best knowledge, only a few theoretical investigations on doped tin clusters were reported, and almost of them focused on a couple of special sizes, namely Sn_nM with $n = 10$ and 12 [23,24,29–32]. Only systemic study was recently carried out on the anionic clusters S_nBi^- by Clayborne et al. [27]. In a consequence, understanding about the growth mechanism and stability motif of doped tin clusters remains in lack. Recently, Lievens and coworkers [33] demonstrated experimentally that the $Sn_{12}Zn$ cluster is a specie

* Corresponding author at: Department of Chemistry, Katholieke Universiteit Leuven, B-3001 Leuven, Belgium.
E-mail address: minh.nguyen@chem.kuleuven.be (M.T. Nguyen).

0301-0104/$ - see front matter © 2011 Elsevier B.V. All rights reserved.
doi:10.1016/j.chemphys.2011.06.041

with enhanced stability, as compared to other small sizes Sn_nZn (n = 2–20). The $Sn_{10}Zn$ cluster was also pointed out to be highly stable, even it is less abundant than the $Sn_{12}Zn$ in the experimental mass spectra. Consequently, these species were assigned to be magic clusters with some novel characters such as a high symmetry structure and a certain aromaticity. However, these interesting characteristics have not been examined by a theoretical study yet.

In this context, motivated by the reasons for the enhanced stability of magic clusters, we set out to perform a systematic theoretical investigation on the zinc-doped tin clusters Sn_nZn (n = 1–12) using quantum chemical methods. The search for the global minima Sn_nZn in each size n is performed using a stochastic search method, recently implemented by us. In order to consider the influence of the Zn-doping, the global minima of the bare clusters Sn_n (n = 1–12) are also re-examined using the same methods. Our calculated results point out that the $Sn_{12}Zn$ and $Sn_{10}Zn$ clusters are indeed enhanced stability species with high binding and embedding energies as well as large HOMO–LUMO gaps. These results offer a rationalization for the experimental observation by mass spectrometric experiment that very high abundance peaks were found at these specific sizes. The growth mechanism of the zinc doped tin clusters is pointed out for the first time and considerably differs from those of the doped group IVA clusters reported previously [16,21,22,19,27].

2. Computational methods

Quantum chemical computations are carried out using the Gaussian 03 [34] and Molpro 06 [35] suites of programs. Geometries and harmonic vibrational frequencies of the low-lying isomers are determined using density function theory with the popular hybrid B3LYP functional, which involves the Becke three-parameter exchange [36], and Lee–Yang–Parr correlation [37] functionals. For smaller size clusters Sn_nZn, with $n \leqslant 7$, the search for the lower-lying isomers is performed manually due to the small number of possible structures to be considered. The initial search for all possible low-lying isomers of each of the larger size Sn_nZn, n from 8 to 12, is performed using a stochastic search algorithm that was recently implemented by us [8]. Let us briefly summary the steps of the search procedure. First, the possible structures of the cluster Sn_nZn are generated by a random "kick" method, and they are then rapidly optimized at the B3LYP/CEP-31G level [38]. In this "kick" procedure, the minimum and maximum distances between atoms are limited to 2 and 7 Å, respectively. Geometries of the stationary points located are then re-optimized using the same B3LYP functional but in conjunction with the LanL2DZ basis set, in which *ab initio* effective core potentials (ECPs) have been generated to replace the Coulomb, exchange and core-orthogonality effects of the chemically inert core electrons in transition metals [39].

In order to obtain more reliable energetic predictions, calculations of single-point electronic energies for the global minima are further performed using the coupled-cluster theory CCSD(T) method [40], making use of the correlation consistent cc-pVTZ-PP basis set, in which PP stands for relativistic pseudo-potentials for metal atoms [41].

The effect of Zn-doping is also evaluated in considering the global minima Sn_n (n = 2–12), whose structures are re-determined at the same B3LYP/LanL2DZ method, and subsequently, calculations of single point electronic energies are also performed using the CCSD(T)/cc-pVTZ-PP method.

3. Results and discussion

3.1. Calibration of computational methods

The lower-lying isomers of the bare clusters Sn_n are re-examined on the basis of the structures previously reported [9,10]. While the shapes, symmetry point groups and electronic states of the global minima Sn_n are summarized in Fig. 1, their HOMO–LUMO gaps and binding energies are given in Table 1. At the B3LYP/LanL2DZ level, our calculated results are in good agreement with earlier reports [9,10]. The $^3\Sigma_g^-$ state is found to be the ground state for the diatomic Sn_2. Its bonding length of 2.715 Å is in line with the experimental value of ~2.74 Å. At the CCSD(T)/cc-pVTZ-PP//B3LYP/LanL2DZ level, the binding energy of $Sn_2(^3\Sigma_g^-)$ of 1.06 eV can be compared to the experimental value of 0.94 eV [42].

Similarly, the CCSD(T) values of binding energies (BE, Table 1) of the oligomers including Sn_3 (D_{3h}), Sn_4 (D_{2h}), Sn_5 (D_{3h}), Sn_6 (C_s) and Sn_7 (D_{5h}) are equal to 1.61, 2.03, 2.19, 2.37 and 2.51 eV, respectively, that are in good agreement with the corresponding experimental values of 1.65, 1.94, 2.11, 2.28 and 2.37 eV [42]. Again the deviations of the calculated parameters are within the chemical accuracy of ±0.1 eV. Accordingly, the computational methods used in this work are effective for determining the energetics of the series of clusters considered.

3.2. Geometries of the low-lying isomers Sn_nZn (n = 1–12) and their growth mechanism

While the shapes, relative energies and symmetry point groups of Sn_nZn, with n ranging from 1 to 12, obtained at the B3LYP/LanL2DZ level, are displayed in Figs. 2–4, their total energy and zero point energy are given in the Supporting information (ESI). The structures described hereafter are denoted by **n.x**, in which **n** stands for the size considered (from 2 to 12), and **x** indicates the *x*th isomer located for this size. As for a convention, structure **n.1** corresponds to the energetically lowest-lying isomer of the size n.

At the B3LYP/LanL2DZ level, the $^3\Sigma$ state is confirmed to be the ground state of the diatomic SnZn with a large singlet–triplet gap of 19.8 kcal/mol.

For the triatomic system, three Sn_2Zn structures are possible, including two linear forms ZnSnSn and SnZnSn, and a triangular

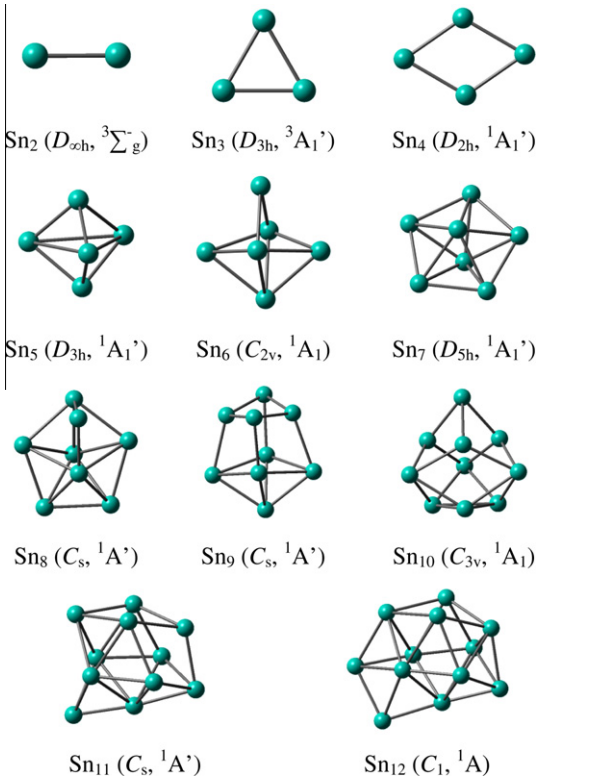

Fig. 1. The shape, symmetry point group and electronic state of the global minima Sn_n, n = 2–12, using B3LYP/LanL2DZ calculations.

Table 1
Binding energies (BEs), embedding energies (EEs) and HOMO–LUMO gaps of the global minima Sn_n and Sn_nZn (n = 1–12) using the CCSD(T)/cc-pVTZ-PP//B3LYP/LanL2DZ level.

Structure	BE (eV)	EE (eV)	HLG (eV)	Structure	BE (eV)	BE(eV)[a]	HLG(eV)
1.1	0.22	0.45	–	–	–	–	–
2.1	0.92	0.63	1.59	Sn_2	1.06	0.94	–
3.1	1.49	1.12	2.39	Sn_3	1.61	1.65	–
4.1	1.66	0.16	1.79	Sn_4	2.03	1.94	2.06
5.1	1.97	0.82	2.14	Sn_5	2.19	2.11	2.51
6.1	2.06	0.17	2.21	Sn_6	2.37	2.28	2.41
7.1	2.20	0.02	2.24	Sn_7	2.51	2.37	2.59
8.1	2.20	0.49	1.99	Sn_8	2.42	–	1.91
9.1	2.35	1.08	2.32	Sn_9	2.49	–	2.09
10.1	2.44	1.00	2.35	Sn_{10}	2.59	–	2.24
11.1	2.41	1.05	1.81	Sn_{11}	2.53	–	1.57
12.1	2.50	2.12	2.74	Sn_{12}	2.53	–	1.64

[a] Experimental values obtained from Ref. [42].

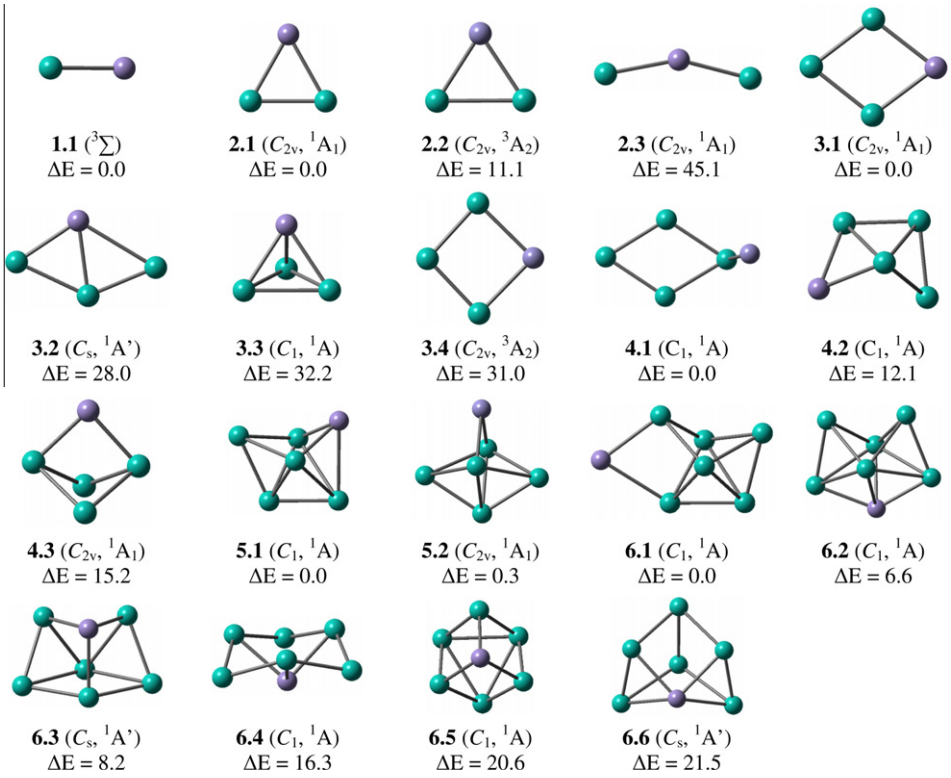

Fig. 2. The shape, symmetry point group, electronic state and relative energy (kcal/mol) of the lower-lying isomers Sn_nZn (n = 2–6) (B3LYP/LanL2DZ + ZPE).

form (Fig. 2). The C_{2v} structure **2.1**, in which Zn connects two Sn atoms of the diatomic Sn_2 is calculated as the global minimum for Sn_2Zn. Both linear forms are not located after optimization and converge to a bent form **2.3**, that is however much less stable than **2.1**. It is interesting to notice that the triplet **2.2** (C_{2v}, $^3A_2$) is quite stable with a relative energy of 11.1 kcal/mol above **2.1**.

For the tetraatomic Sn_3Zn system, three isomers are obtained, including both planar **3.1** and **3.2**, and a three-dimensional **3.3** structures. In the latter, Zn is doped on the C_3 axis of the triangular Sn_3 (D_{3h}) (Fig. 2). At the B3LYP/Lan2LDZ level, **3.1** (C_{2v}) is the most stable isomer. The three Sn–Sn distances of **3.1** are close and vary in the range of 2.815–3.452 Å. Thus **3.1** can be regarded as a doped structure in which Zn connects with two Sn atoms of the triangular Sn_3 rather than a substituted structure on the basis of the rhombic form Sn_4 (D_{2h}) in which the distances of Sn atoms sitting on the same symmetry axis are quite different from the others. A distorted structure **3.2**, that is formed by substituting one Sn atom of the rhombic Sn_4 by Zn is the next isomer with a relative energy of 28.0 kcal/mol. The three-dimensional **3.3** is much less stable. As shown in Fig. 2, a triplet state **3.4** (C_{2v}, $^3A_2$) is also located for Sn_3Zn, but it is substantially higher in energy than **3.1**.

For the pentaatomic Sn_4Zn, we find the C_1 structure **4.1**, in which Zn binds to one Sn atom of the rhombic Sn_4 (D_{2h}) to be the global minimum. In **4.2**, Zn connects with two Sn atoms of Sn_4 and turns out to be the second-lying isomer with a relative energy of 12.1 kcal/mol. The C_{2v} structure **4.3**, whose shape is the global minimum of the Ge_4Zn congener, is found to be next isomer with 15.2 kcal/mol higher.

Similarly, **5.1** (C_1) which is formed by capping Zn on a triangular surface of the Sn_5 (D_{3h}) cluster, is the global minimum of the Sn_5Zn system. Although the C_{2v} structure **5.2** is located with low relative energy, it is actually a transition structure containing one imaginary frequency.

In the most stable isomer **6.1** (C_1) for Sn_6Zn, the Zn atom connects two Sn atoms of the Sn_6 (C_{2v}) host. **6.2** (C_{2v}), in which one Sn atom of the pentagonal bipyramid Sn_7 clusters is substituted by Zn, is the next isomer with a relative energy of 6.6 kcal/mol.

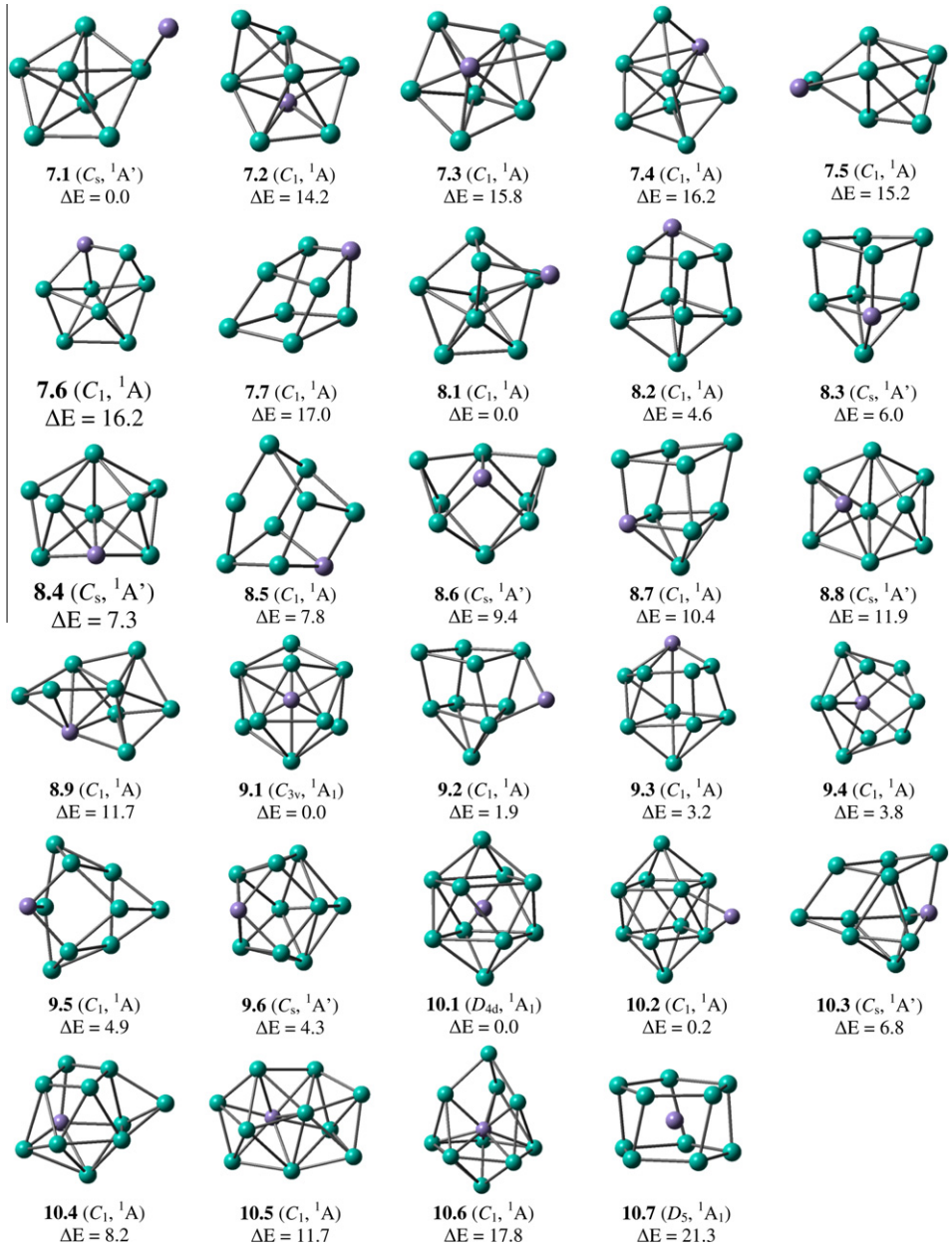

Fig. 3. The shape, symmetry point group, electronic state and relative energy (kcal/mol) of the lower-lying isomers Sn_nZn (n = 7–10) (B3LYP/LanL2DZ + ZPE).

While **6.3** (C_s) is also of low energy, the others are much less stable being at least ~16 kcal/mol higher in energy than **6.1**.

Various structures of the Sn_7Zn system are formed by either binding Zn to the Sn_7 host, or substituting one Sn of the Sn_8 minimum by Zn (Fig. 3). In the most stable isomer **7.1** (C_s), Zn binds to one Sn atom of the heptagonal bipyramid Sn_7. Thus, the substituting motif based on the Sn_8 background, is less favored in this case. Other possible structures, from **7.2** to **7.7**, formed by substituting one Sn atom of Sn_8 by Zn are less favored lying at least ~14 kcal/mol above **7.1**.

Similar to Sn_7Zn, the main feature of the global minimum **8.1** (C_1) is that Zn is doped on a surface of the related Sn_8 cluster. However, two structures **8.2** (C_1, ^{1}A) and **8.3** (C_s, ^{1}A′) that are formed by substituting one Sn atom of the Sn_9 minimum by Zn at different positions also turn out to be quite stable being 4.6 and 6.0 kcal/mol higher in energy, respectively. Other structures based on a Sn_9 background, from **8.4** to **8.9**, are close in energy content, and being at least ~7 kcal/mol less stable than **8.1**.

There is a competition in relative energy between the possible exohedral and endohedral forms in the Sn_9Zn clusters. Two structures, including the C_{3v} **9.1**, in which Zn is located at the center of a Sn_9 (C_{3v}) cage, and the C_1 **9.2** which dopes Zn outside Sn_9 cage, are nearly degenerate with energy difference of ~2 kcal/mol. Substitution of one Sn atom at various positions of the Sn_{10} minimum results in quite stable structures (from **9.3** to **9.7**), whose relative energies are close to each other as shown in Fig. 3.

Similar features are observed for $Sn_{10}Zn$. Two structures **10.1**(D_{4d}, ^{1}A$_1$) where Zn is located at the center of a Sn_{10} (D_{4d}) cage, and **10.2** (C_1, ^{1}A) where Zn is doped outside the Sn_{10} cage, are again energetically degenerate. The remaining forms are less stable with at least ~7 kcal/mol above **10.1** (Fig. 3).

It is remarkable that the mechanism of exohedral doping is abruptly interrupted at the size n = 11 where the cluster forms an encapsulated structure **11.1** (C_{2v}, ^{1}A$_1$). In the latter, Zn is endohedrally doped inside the Sn_{11} cage (Fig. 4). Such a behavior is similar to that of the $Ge_{11}Zn$ and $Ge_{11}Cu$ systems. Most of the

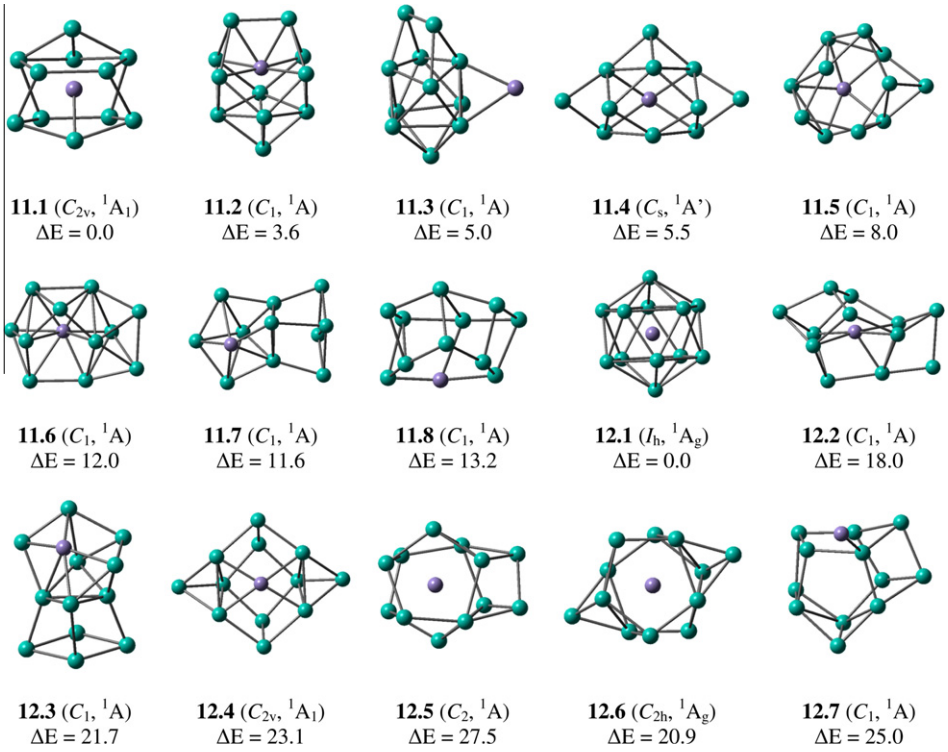

Fig. 4. The shape, point group, electronic state and relative energy (kcal/mol) of the low-lying isomers Sn_nZn (n = 11–12) using the B3LYP/LanL2DZ + ZPE level.

lower-lying isomers of $Sn_{11}Zn$, that are formed either by doping Zn into the Sn_{11} host (from **11.2** to **11.5**), or by substituting a Sn by Zn of the Sn_{12} background (from **11.6** to **11.8**), are found to be significantly less stable.

As expected from the experimental observations on zinc-doped tin clusters,[33] the icosahedral structure (I_h) **12.1** is confirmed to be the global minimum for $Sn_{12}Zn$. The remaining forms are at least ~18 kcal/mol higher in energy.

In general, two different growth mechanisms can be clearly observed here. For the series of small clusters Sn_nZn, with $n \leqslant 8$, the global minima Sn_nZn are generated by capping Zn on surfaces of the Sn_n hosts. A competition in relative energy between both exohedral and endohedral types of structure actually occurs at the sizes of 9 and 10 where the endohedral ones turn out to be more favored. For the larger clusters with n = 11 and 12, the encapsulated structures in which Zn is endoherally doped into the Sn_n cages become dominant. Compared to the previous theoretical studies on doped germanium clusters, the doped tin clusters present a different growth pattern. The global minima of the small clusters Ge_nZn and Ge_nCu ($n \leqslant 8$) are formed through a substitution mechanism in which one Ge of the Ge_{n+1} minimum is replaced by Zn [22]. In contrast, as discussed above, the small Sn_nZn clusters arise from a capping of Zn on the surface of the Sn_n host, with $n \leqslant 8$, and the endohedrally doped structures become predominant from n = 9 to 12.

3.3. Relative stability of clusters

Attempts have in fact been made to define a sole parameter characterizing the relative stabilities of the clusters. However, it appears that such stability can better be quantified from a set of different parameters. Here we use the average binding energy (*BE*), embedding energy (*EE*), frontier orbital energy gap and second order difference in the total energies (Δ^2E). Additionally, doping the impure Zn into the Sn_n host also has influence on the relative stability of the binary clusters Sn_nZn. The calculated energetic values for both pure Sn_n and impure Sn_nZn clusters provide some insights into such influence.

The average binding energy (E_b) and the second order difference in the total energies (Δ^2E) of pure Sn_n and Zn-doped Sn_nZn clusters are defined as follows.

For pure clusters Sn_n, using the reaction $Sn_n \rightarrow n$Sn, we define E_b as:

$$E_b(Sn_n) = [nE(Sn) - E(Sn_n)]/n \quad (1)$$

$$\Delta^2E(Sn_n) = E(Sn_{n-1}) + E(Sn_{n+1}) - 2E(Sn_n) \quad (2)$$

For impure clusters Sn_nZn, using the reaction using the reaction $Sn_nZn \rightarrow n$Sn + Zn, we define E_b as:

$$E_b(Sn_nZn) = [nE(Sn) + E(Zn) - E(Sn_nZn)]/(n+1) \quad (3)$$

$$\Delta^2E(Sn_nZn) = E(Sn_{n-1}Zn) + E(Sn_{n+1}Zn) - 2E(Sn_nZn) \quad (4)$$

where $E(Sn_n)$ and $E(Sn_nZn)$ are total energies of pure Sn_n and impure Sn_nZn clusters, respectively. E(Sn) and E(Zn) are total energies of Sn and Zn atoms, respectively. Number n counts for number of Sn-atoms in the cluster considered.

While the values of average binding energy (E_b) of the global minima Sn_n and Sn_nZn at the CCSD(T)/cc-pVTZ-PP level are given in Table 1, the curves showing the size dependence of these values are displayed in Fig. 5a. The binding energy of the pure cluster Sn_n increases with increasing size and attains a maximum peak at n = 10, and then it slightly decreases as n > 10. A local maximum peak is found at n = 7. This trend is consistent with the previous reports that both Sn_{10} and Sn_7 are the enhanced stability species in the series of small tin clusters. On other hand, the binding energy of the Zn-doped clusters Sn_nZn increases continuously and attains the first peak at n = 10, and then the highest BE value is obseved at n = 12. Our calculated results are thus consistent with the mass spectrometric experiment that the $Sn_{12}Zn$ size corresponds to the most abundance, and $Sn_{10}Zn$ is also of high stability. One should note that the Zn doping slightly decreases the binding energy of the impure clusters Sn_nZn, as compared to those of the host Sn_n.

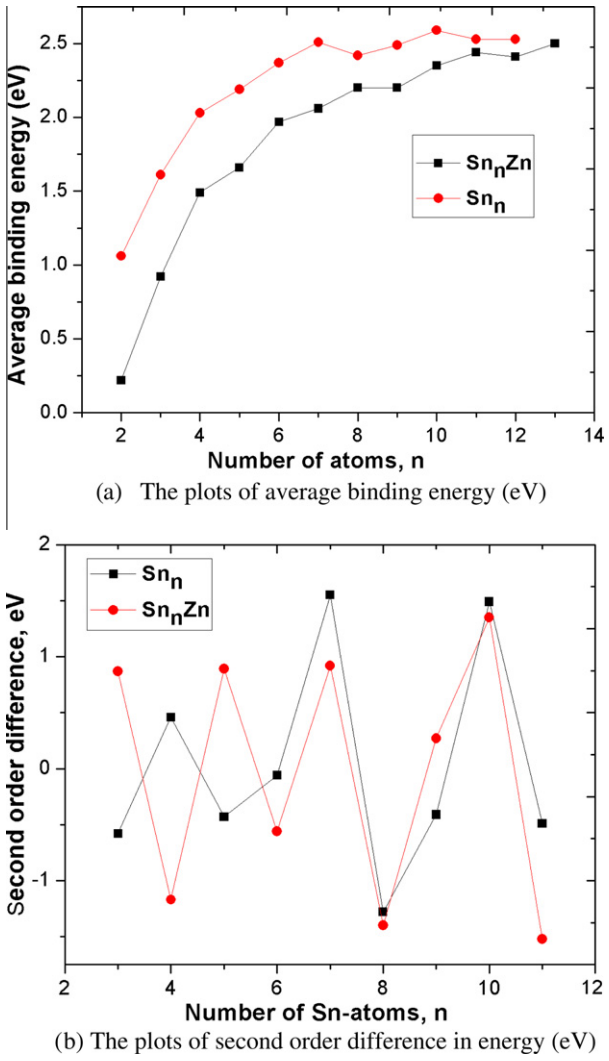

Fig. 5. The plots of (a) average binding energy and (b) second order difference in energy of the Sn_n and Sn_nZn clusters.

The binding energy of 0.22 eV of the diatomic SnZn at the CCSD(T)/cc-pVTZ-PP level, is much smaller than the value of 1.06 eV of the dimer Sn_2. Consequently, the weaker bonding strength of the Sn–Zn bond can be considered as the main reason for the lower binding energies of the mixed Sn_nZn clusters with respect to the bare hosts.

Similar trends are found for the plots of second order difference (Δ^2E) in total energy in both series of pure Sn_n and impure Sn_nZn clusters (Fig. 5b). For Sn_n, two maximum peaks emerge at the sizes of 7 and 10, that are again consistent with the binding energy behavior. As a consequence, the clusters Sn_7 and Sn_{10} are confirmed to be the species of enhanced stability. In the case of Zn-doped tin clusters, a maximum peak is again observed at the size of 10, followed by the lowest value at the size of 11.

Because of the high stability of the endohedral structures Sn_nZn having $n \geqslant 9$, evaluation of the embedding energy (EE) is necessary. Embedding energy (EE) can be considered as the energy released upon doping Zn into the Sn_n cages, and defined as follows using the reactions $Sn_nZn \rightarrow Sn_n + Zn$:

$$EE(Sn_nZn) = E(Sn_n) + E(Zn) - E(Sn_nZn) \quad (5)$$

A high EE value indicates a strong interaction between Zn and the host Sn_n, and consequently leads to a high thermodynamical stability of the relevant Sn_nZn cluster. Table 1 points out that the EE values of small clusters are quite small, with size $n \leqslant 8$, and they steady increase up to ~1.00 eV at $n = 9$, 10 and 11. Such an increase can be understood because the endohedral structures become more dominant from size $n = 9$. It is remarkable that the EE value of the $Sn_{12}Zn$ (I_h) amounts to 2.12 eV that is very high as compared to those of the other sizes. This result indicates that $Sn_{12}Zn$ bears an enhanced stability, in consistence with the above discussion.

3.4. HOMO–LUMO gaps

The frontier orbitals gap is usually considered as a measure of kinetic stability of compounds. A large gap indicates that the compound is more inert with respect to chemical reactions. Results given in Table 1 reveal that the HOMO–LUMO gaps of small tin clusters Sn_n with $n \leqslant 7$ is slightly larger than those of corresponding zinc doped tin clusters Sn_nZn. However, an opposite trend is observed for the larger sizes ($n \geqslant 8$). The HOMO–LUMO gap of $Sn_{12}Zn$ cluster is equal to 2.7 eV, being the largest gap as compared to those of the other sizes. Furthermore, this is also remarkably higher than the value of 1.6 eV of the pure Sn_{12}. Thus, doping Zn into the Sn_{12} cage improves considerably the stability of the resulting icosahedral cluster $Sn_{12}Zn$. In a consistence with the discussion above, the $Sn_{10}Zn$ species (D_{4d}) also shows a large gap of 2.4 eV. Overall, the effect of magic stabilities is basically manifested by the high abundance experimental observation of the corresponding sizes.

3.5. Electronic structure and electronic shell model

A system with enhanced stability usually exhibits novel characteristics such as a large degree of aromaticity, highly symmetrical and compact structure, and satisfies electronic shell models as much as possible. As observed from experiment, the icosahedral $Sn_{12}Zn$ (I_h) and $Sn_{10}Zn$ (D_{4d}) forms are found to possess an enhanced stability within the series of small Sn_nZn clusters. Accordingly, a detailed analysis of electronic structure and aromaticity of these species is of significant interest.

According to a simple electronic shell model, in which the valence electrons are assumed to freely itinerant in a simple mean-field potential formed by the nuclei of atoms [43], the valence electrons fill the spherical orbitals of a system according to the pattern of $1S^21P^61D^{10}2S^21F^{14}2P^61G^{18}2D^{10}$, etc. Consequently, the number of electrons of 8, 20, 34, 40, 58, 68... are proposed to be the magic numbers, that all correspond to the closed shell electrons. However, recent experimental and theoretical investigations clearly demonstrated that the number of 50 electrons also constitutes a magic number for the enhanced stability systems [17,44,45]. This special stability is rationalized by the fact that a splitting of the $l = 4$ (F) shells in an icosahedral symmetry lowers the energy under crystal field effects [44]. This assumption was subsequently applied to the high stability cationic $Pb_{12}Al^+$ cluster [45], and the systems of 50 valence electrons $Ge_{12}M^x$, with M = Li, Na, Be, Mg, B, Al, and $x = -1$, 0, +1 [17].

Due to the high symmetry of an icosahedral structure (Fig. 6), the MOs of $Sn_{12}Zn$ strongly resemble the spherical harmonics, but with significant variations. The MOs shape and their energy levels indicate that the 50 valence electrons of the icosahedron $Sn_{12}Zn$ (I_h) are distributed in an energy ordering of [$1S^21P^6$ $1D^{10}$ $1F^6$ $2S^2$ $1F^8$ $2P^6$ $1G^{10}$]. The lowest-lying MO is an s-type valence orbital, that is followed by a triply degenerate p-type $1P^6$ subshell, a 5-times degenerate d-type subshell $1D^{10}$. The 1F subshell is split into a threefold T_{2u} and a fourfold G_u degenerate levels, while the 1G subshell is split into a fivefold H_g and a fourfold G_g degenerate levels. This ordering of energy levels is similar to those of $Pb_{12}Al^+$ and $Ge_{12}M^x$ [17,45]. Accordingly, the icosahedral $Sn_{12}Zn$ (I_h) is expected to be a magic cluster that satisfies well the electronic shell model.

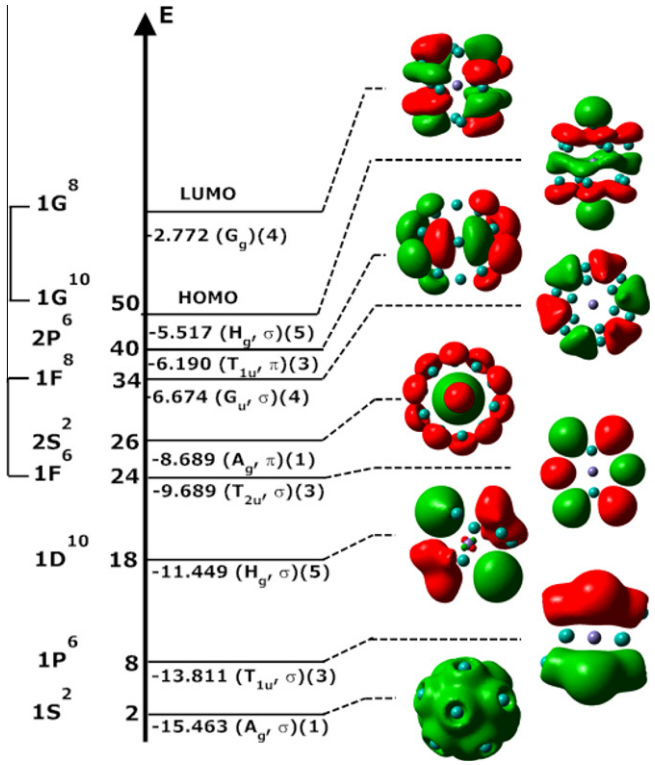

Fig. 6. Energy levels and orbitals of the icosahedral structure $Sn_{12}Zn$ (I_h) (B3LYP/LanL2DZ).

3.6. Spherical aromaticity

While the classical Hückel rule of $(4n + 2)$ π electrons is usually applied to probe the aromatic character of planar structures, the I_h symmetrical fullerenes were reported to have spherical aromaticity through a $2(N + 1)^2$ count, that was recently proposed by Hirsch and coworkers [46]. The π-electron system of these species can approximately be considered as a spherical electron gas, which surrounds the surface of a sphere. The wave functions of this electron gas can be characterized by the angular momentum quantum numbers (l = 0, 1, 2, 3, ...) that are comparable to the atomic s, p, d, f, ... orbitals. According to the classical Pauli principle, if a system with $2(N + 1)^2$ π-electrons fully fills all π-shells, it then exhibits aromaticity.

The pictures of the densities of states of $Sn_{12}Zn$ shown in Fig. 6 reveals two orbital sets: the first containing the MOs of 1S (A_g, σ), 1P (T_{1u}, σ), 1D (H_g, σ), 1F (T_{2u}, σ) 1F (G_u, σ), 1G (H_g, σ) are occupied by 42 σ-electrons, while the second set including the MOs of 2S (A_g, π) and 2P (T_{1u}, π) are occupied by 8 valence π-electrons. Consequently, this π electron system makes $Sn_{12}Zn$ aromatic that is consistent with a $2(N + 1)^2$ count.

A similar observation is found for the $Sn_{10}Zn$ that is also a structure having an enhanced stability in the small series The shapes of the relevant MO of the $Sn_{10}Zn$ (D_{4d}) (Fig. S1, ESI) reveal that its 42 valence electrons are distributed into two orbital sets: the first is occupied by 34 σ-electrons, whereas the second set contains the MOs of 2S (A_1), 2P (B_2) and 2P (E_1) and is thus occupied by 8 π-electrons. As a consequence, the $Sn_{10}Zn$ can also be established as a spherical aromaticity system bearing 8 valence π-electrons.

4. Concluding remarks

We carried out a systematic investigation on a series of small zinc doped tin clusters Sn_nZn ($n = 1–12$) using both DFT and CCSD(T) methods. The search for the low-lying isomers is performed using a stochastic searching method that we have recently implemented. The following points emerge from our calculated results:

(i) The global minima are firmly established, and the growth pattern of the binary clusters can be formulated as follows: (i) the small clusters Sn_nZn with $n \leqslant 8$ are formed by capping Zn onto the surface of the global minimum of Sn_n ; (ii) a competition between exohedral and endohedral structures appears at the sizes of 9 and 10, in which the endohedral structures tend to be consistently favored; (iii) for the larger clusters with $n = 11$ and 12, the clusters are taking shape by encapsulating Zn into the empty cages Sn_n.

(ii) While the binding energy of the Sn_nZn clusters are slightly smaller than those of host Sn_n due to the inherently weak bonding strength of the diatomic Sn–Zn, the frontier orbital energy gaps of the clusters Sn_nZn, with $n = 8–12$, are found to be larger than those of their parent Sn_n. An interesting feature is that the icosahedral $Sn_{12}Zn$ (I_h) turns out to be a magic cluster with large HOMO–LUMO gap, high binding and embedding energies, that is consistent with experiment. The $Sn_{10}Zn$ (D_{4d}) system is also found to be a highly stable system.

(iii) Both the $Sn_{12}Zn$ and $Sn_{10}Zn$ clusters exhibit a spherically aromatic character with 8 valence π-electrons, that satisfies the electron counting rule of $2(N + 1)^2$, the enhanced stability of the icosahedral $Sn_{12}Zn$ (I_h) can also be rationalized by its closed crystal field splitting shell.

Acknowledgements

The authors are indebted to the K.U.Leuven Research Council for continuing support (GOA, IDO and IUAP programs). T.B.T. thanks the Arenberg Doctoral School for a scholarship. M.T.N. thanks the ICST of HoChiMinh City for supporting his stays in Vietnam.

Appendix A. Supplementary data

Supplementary data associated with this article can be found, in the online version, at doi:10.1016/j.chemphys.2011.06.041.

References

[1] F. Baletto, R. Ferrando, Rev. Mod. Phys. 77 (2005) 371.
[2] E.C. Honea, A. Ogura, C.A. Murray, K. Raghavachari, W.O. Sprenger, M.F. Jarrold, W.L. Brown, Nature 366 (1993) 42.
[3] T.P. Martin, H. Schaber, J. Chem. Phys. 83 (1985) 855.
[4] S. Nigam, C. Majumder, S.K. Kulshreshtha, J. Chem. Phys. 121 (2004) 7756.
[5] J.T. Lyon, P. Gruene, A. Fielickke, G. Meijer, E. Janssens, P. Claes, P. Liewens, J. Am. Chem. Soc. 131 (2009) 1115.
[6] E. Kikuchi, S. Ishii, K. Ohno, Phys. Rev. B 74 (2006) 195410.
[7] (a) S. Yoo, X.C. Zeng, J. Chem. Phys. 124 (2006) 184309;
(b) S. Bulusu, S. Yoo, Z.C. Zeng, J. Chem. Phys. 122 (2005) 164305.
[8] T.B. Tai, M.T. Nguyen, J. Chem. Theory Comput. 7 (2011) 1119.
[9] (a) S. Schafer, B. Assadollahzadeh, M. Mehring, P. Schwerdtfeger, R. Schafer, J. Phys. Chem. A 112 (2008) 12312;
(b) B. Assadollahzadeh, S. Schafer, P. Schwerdtfeger, J. Comput. Chem. 31 (2010) 929.
[10] (a) K. Balasubramanian, K.S. Pitzer, J. Chem. Phys. 78 (1983) 321;
(b) K. Balasubramanian, J. Chem. Phys. 85 (1986) 3401;
(c) C. Zhao, K. Balasubramanian, J. Chem. Phys. 115 (2001) 3121;
(d) D. Dai, K. Balasubramanian, J. Chem. Phys. 96 (1992) 8345;
(e) D. Dai, K. Balasubramanian, J. Phys. Chem. 100 (1996) 19321.
[11] (a) C. Majumder, V. Kumar, H. Mizuseki, Y. Kawazoe, Phys. Rev. B 71 (2005) 035401;
(b) C. Majumder, V. Kumar, H. Mizuseki, Y. Kawazoe, Phys. Rev. B 64 (2001) 233405.
[12] L.F. Cui, L.M. Wang, L.S. Wang, J. Chem. Phys. 126 (2007) 064505.
[13] C. Rajesh, C. Majumder, M.G.R. Rajan, S.K. Kulsheshtha, Phys. Rev. B 72 (2005) 235411.

[14] B.L. Wang, J.J. Zhao, X.S. Chen, D.N. Shi, G.H. Wang, Phys. Rev. A 71 (2005) 033201.
[15] X.P. Li, W.C. Lu, Q.J. Zang, G.J. Chen, C.Z. Wang, K.M. Ho, J. Phys. Chem. A 113 (2009) 6217.
[16] (a) G. Gopakumar, P. Lievens, M.T. Nguyen, J. Chem. Phys. 124 (2006) 214312;
(b) G. Gopakumar, P. Lievens, M.T. Nguyen, J. Phys. Chem. A 111 (2007) 4355;
(c) X.J. Hou, G. Gopakumar, P. Lievens, M.T. Nguyen, J. Phys. Chem. A 111 (2007) 13544;
(d) G. Gopakumar, V.T. Ngan, P. Lievens, M.T. Nguyen, J. Phys. Chem. A 112 (2008) 12187;
(e) G. Gopakumar, X. Wang, L. Lin, J. de Haeck, P. Lievens, M.T. Nguyen, J. Phys. Chem. C 113 (2009) 10856.
[17] (a) T.B. Tai, M.T. Nguyen, Chem. Phys. Lett. 492 (2010) 290;
(b) T.B. Tai, M.T. Nguyen, Chem. Phys. Lett. 502 (2011) 187;
(c) T.B. Tai, M.T. Nguyen, J. Phys. Chem. C. (2011), doi:10.1021/jp111324n.
[18] J. Wang, L. Ma, J. Zhao, G. Wang, J. Phys: Condens. Matter. 20 (2008) 335223.
[19] Z.J. Li, K.H. Su, Theor. Chem. Acc. 124 (2009) 345.
[20] G.A. Breaux, D.A. Hillman, C.M. Neal, M.F. Jarrold, J. Phys. Chem. A 109 (2005) 8755.
[21] D. Bandyopadhyay, P. Sen, J. Chem. Phys. A 114 (2010) 1835.
[22] (a) J. Wang, J.G. Han, J. Chem. Phys. 123 (2005) 244303;
(b) J. Wang, J.G. Han, Chem. Phys. 342 (2007) 253.
[23] (a) V. Kumar, Y. Kawazoe, Appl. Phys. Lett. 83 (2003) 2677;
(b) V. Kumar, Y. Kawazoe, Appl. Phys. Lett. 80 (2002) 859;
(c) V. Kumar, A.K. Singh, Y. Kawazoe, Nano. Lett. 4 (2004) 677.
[24] Z. Chen, S. Neukermans, Z. Wang, E. Janssens, Z. Zhou, R.E. Silverans, R.B. King, P.v.R. Schleyer, P. Lievens, J. Am. Chem. Soc. 128 (2006) 12829.
[25] L.F. Cui, X. Huang, L.M. Wang, J. Li, L.S. Wang, Angew. Chem., Int. Ed. 46 (2007) 742.
[26] J. Lu, S. Nagase, Chem. Phys. Lett. 372 (2003) 394.
[27] P.A. Clayborne, U. Gupta, A.C. Reber, J.J. Melko, S.N. Khana Jr., A.W. Castleman, J. Chem. Phys. 133 (2010) 134302.
[28] E.N. Esenturk, J. Fettinger, B. Eichhorn, J. Am. Chem. Soc. 128 (2006) 9178.
[29] J.M. Matxain, M. Piris, E. Formoso, J.M. Mercero, X. Lopez, J.M. Ugalde, ChemPhysChem 8 (2007) 2096.
[30] X. Chen, K. Deng, Y. Liu, C. Tang, Y. Yuan, W. Tan, X. Wang, J. Chem. Phys. 129 (2008) 094301.
[31] A.K. Kandalam, G. Chen, P. Jena, Appl. Phys. Lett. 92 (2008) 143109.
[32] L.F. Cui, X. Huang, L.M. Wang, D.Y. Zubarev, A.I. Boldyrev, J. Li, L.S. Wang, J. Am. Chem. Soc. 128 (2006) 8930.
[33] S. Neukermans, X. Wang, N. Veldeman, E. Janssens, R.E. Silverans, P. Lievens, Int. J. Mass. Spec. 252 (2006) 145.
[34] M.J. Frisch et al., Gaussian, Inc., Wallingford, CT, 2004.
[35] H.J. Werner, et al., Molpro, version 2008.1.
[36] A.D. Becke, J. Chem. Phys. 98 (1993) 5648.
[37] C. Lee, W. Yang, R.G. Parr, Phys. Rev. B. 37 (1988) 785.
[38] W.J. Stevens, M. Krauss, H. Basch, P.R. Jasien, Can. J. Chem. 70 (1992) 612.
[39] P.J. Hay, W.R. Wadt, J. Chem. Phys. 82 (1985) 270.
[40] R.J. Bartlett, M. Musial, Rev. Mod. Phys. 79 (2007) 291. and references therein.
[41] K.A. Peterson, J. Chem. Phys. 119 (2003) 11099.
[42] K.A. Gingerich, A. Desideri, D.L. Cocke, J. Chem. Phys. 62 (1975) 731.
[43] M. Brack, Rev. Mod. Phys. 65 (1993) 677.
[44] K.E. Schriver, J.L. Persson, E.C. Honea, R.L. Whetten, Phys. Rev. Lett. 64 (1990) 2539.
[45] S. Neukermans, E. Janssens, Z.F. Chen, R.E. Silverans, P.v.R. Schleyer, P. Lievens, Phys. Rev. Lett. 92 (2004) 163401.
[46] A. Hirsch, Z. Chen, H. Jiao, Angew. Chem., Int. Ed. 39 (2000) 3915.